A Pixel to Pixel Hyperspectral Synthetic Image Model Inter-Comparison Study

Charles R. Bostater, Jr.[1], Luce Bassetti [2]
Marine Environmental Optics Laboratory & Remote sensing Center
College of Engineering, Florida Institute of Technology

ABSTRACT

The purpose of this paper is to present simulation results comparing e a Monte Carlo Hyperspectral Simulation Model (MCHSIM) which generates synthetic images with realistic water wave surface to an iterative layered radiative transfer model used to generate hyperspectral synthetic images with realistic water wave surfaces. The Monte Carlo model is divided into 5 steps: (1) generation of the photons, (2) tracking of the photon optical path and simultaneously (3) recording of the photon's location within the water column, (4) a tabulation of the photon location or positions, and conversion to meaningful radiometric quantities and (5) a calculation and processing of the event probabilities between successive photons. This model will was compared to the ILRT which is analytical and uses an iterative method to converge on the solution to the layered two flow radiative transfer model. Overall, the purpose of this research is to develop a better scientific understanding of the influence of the air-sea interface on the remote sensing signal from 400 to 750 nm, as well as the coupled influence of water waves and shallow bottom reflectance effects from benthic aquatic habitat features such as submerged vegetation, corals, and other objects submerged within the water column. Results suggest that the two models are comparing quite well when pixel reflectance data are compared as shown in the 2 dimensional plots. Additional model simulations and comparisons are needed in order for the research to result in practical applications for algorithm development of coastal water quality indicators.

Keywords: hyperspectral remote sensing, water waves, synthetic images, modeling, simulation, radiative transfer, monte carlo modeling, water surface reflectance.

1. BACKGROUND

The Analytical Model for Synthetic Image Generation

An evaluation of the iterative model used and reported below was first accomplished by Bostater and Huddleston (2202). The motivation of such work was two model radiation transfer in coastal waters. The modified two flow equations were used in order to create fast and accurate estimates of light disctributions in a layered media. Applying specific boundary conditions the final equations for upwelling and downwelling irradiance were shown and used in this research as:[1]

[1]Dr Charles R. Bostater, Jr. bostater@probe.ocn.fit.edu; phone 321-674-7113; fax 321-773-0980; Center for Remote Sensing, Marine and Environmental Optics Laboratory, 150 West University Blvd., Melbourne, FL, USA 32901 (address correspondence the above author.)
[2] Luce Bassetti, lbassetti@hpa.com; phone 813-876-6800; fax 813-876-6700; now at Halcrow HPA 4010 Bay Scout Blvd Suite 580, Tampa. FL,USA, 33607

Remote Sensing of the Ocean, Sea Ice, and Large Water Regions 2006,
edited by Charles R. Bostater, Jr., Xavier Neyt, Stelios P. Mertikas, Miguel Vélez-Reyes,
Proc. of SPIE Vol. 6360, 636008, (2006) · 0277-786X/06/$15 · doi: 10.1117/12.692614

$$E_d(z,i) = \left[\begin{array}{l} \dfrac{(\psi(i) - a(i) - b(i)}{2\psi(i)} e^{\psi(i)z(i)} \\ + \dfrac{(\psi(i) - a(i) - b(i)}{2\psi(i)} e^{-\psi(i)z(i)} \end{array} \right] E_d(0,i) \qquad (1)$$

$$+ \left[\frac{b(i)}{2\psi(i)} \left(e^{\psi(i)z(i)} + e^{-\psi(i)z(i)} \right) \right] E_u(0,i)$$

$$+ \left[\begin{array}{l} \dfrac{(c(i) - m(i)\alpha(i)}{2\psi(i)} \left(e^{\psi(i)z(i)} - e^{-\psi(i)z(i)} \right) \\ + 2\psi(i) e^{-\alpha(i)z(i)} \end{array} \right] E_s(0,i).$$

where:

$E_d(z,i)$ = hemispherical downwelling vector irradiance at depth z in layer i for a layered water column (W m^{-2}),

$E_d(0,i)$ = hemispherical downwelling vector irradiance at surface in layer i for a layered water column (W m^{-2}),

$E_u(0,i)$ = hemispherical upwelling vector irradiance at surface in layer i for a layered water column (W m^{-2}),

$E_s(0,i)$ = hemispherical collimated vector irradiance at surface in layer i for a layered water column (W m^{-2}),

$a(0,i)$ = total absorption coefficient of layer i for a layered water column (m^{-1}),

$b(0,i)$ = total backscattering coefficient of layer i for a layered water column (m^{-1}),

$c(0,i)$ = specular irradiance conversion coefficient for downwelling diffuse irradiance in layer "i" in the,

$\alpha(0,i)$ = diffuse beam attenuation coefficient of layer i in a layered water column,

$m(0.i)$ = particular solution for downwelling constant of layer i in a layered water column diffuse beam attenuation coefficient of layer i in a layered water column (m^{-1}),

$n(i)$ = particular solution for upwelling constant of layer I in a layered water column,

$\psi(i) = \sqrt{a^2 + 2ab}$ a second order attenuation coefficient for a layer i in the homogeneous water column or water layer,

and,

$$E_u(0,i) = \left[\begin{array}{l} \dfrac{\psi(i) - a(i) - b(i)}{2\psi(i)} e^{\psi(i)z(i)} \\ + \dfrac{\psi(i) - a(i) - b(i)}{2\psi(i)} e^{-\psi(i)z(i)} \end{array} \right] E_u(z,i)$$

$$+ \left[\frac{b(i)}{2\psi(i)} \left(e^{\psi(i)z(i)} + e^{-\psi(i)z(i)} \right) \right] E_d(0,i)$$

$$+ \left[\frac{c(i) - m(i)\alpha(i)}{2\psi(i)} \left(e^{\psi(i)z(i)} - e^{-\psi(i)z(i)} \right) \right] E_s(z,i)$$

$$+ \left[\begin{array}{l} \dfrac{n(i)}{2\psi(i)} \left[\begin{array}{l} \left(2\psi(i) - \psi(i) e^{-\alpha(i)z(i)} \right) \\ * \left(e^{\psi(i)z(i)} - e^{\psi(i)z(i)} \right) \end{array} \right] \\ - \alpha(i) e^{-\alpha(i)z(i)} \left(\begin{array}{l} e^{\psi(i)z(i)} \\ - e^{-\psi(i)z(i)} \end{array} \right) \end{array} \right] E_s(0,i)$$

where:

$E_u(z,i)$ = hemispherical upwelling vector irradiance at depth z in layer i for a layered water column (W m^{-2}),
$E_s(z,i)$ = hemispherical collimated vector irradiance at depth z in layer i for a layered water column (W m^{-2}),
$E_d(0,i)$ = hemispherical downwelling vector irradiance at surface in layer i for a layered water column (W m^{-2}),
$E_u(0,i)$ = hemispherical upwelling vector irradiance at surface in layer i for a layered water column (W m^{-2}),
$E_s(0,i)$ = hemispherical collimated vector irradiance at surface in layer i for a layered water column (W m^{-2}),
a(i) = total absorption coefficient of layer i for a layered water column (m^{-1}),
b(i) = total backscattering coefficient of layer i for a layered water column (m^{-1}),
c(i) = specular irradiance coefficient for convertion of downwelling diffuse irradiance in "i",
α (i)=diffuse beam attenuation coefficient of layer i ,
m(i) = particular solution for the downwelling irradiance in layer i
n(i) = particular solution for upwelling constant of layer i,
ψ (i) = $\sqrt{a^2 + 2ab}$ a second order attenuation coefficient for a layer i.

These equations form the basis of the iterative model for multiple layers used in the research conducted by Bostater and al. since 2002 and in the results shown below.

Hyperspectral Monte Carlo Model

This model has the unique capability for calculating water surface reflectance values in each pixel of the domain of study. The model was first developed by Bostater and Gimond (2002) for a water column and Bostater and Chiang (2002) utilized the model to generate realistic synthetic images, and is divided into 5 steps:

(1) Generation of the photons,
(2) tracking of the photon optical path and simultaneously,
(3) recording of the photon's location within the water column,
(4) tabulation of the sampling and its conversion to meaningful radiometric quantities and finally,
(5) calculation and processing of the event probabilities between successive photons and their interaction

This innovative model created by Bostater et al. (2002), is a "hyperspectral" 3-D MC model and allows for simulating the influence of bottom reflectance effects and constituents in the water column, as well as estimation of shape factors and mean cosines within a synthetic image scene. The model has been calibrated and tested by Bostater et al., 2002. The MC methods utilize a series of probabilistic events. Each of them is determined by probability distribution functions (pdf's) and associated cumulative frequency distribution (cdf's) or equations in conjunction with uniform random number generators in order to simulate radiative transfer in water (Davies et al., 1995).

2. METHODS

The purpose of this paper is to present simulation results in order to compare a Hyperspectral Monte Carlo Model (MC) which generates synthetic images with realistic water wave surfaces to an iterative layered radiative transfer model used to generate hyperspectral synthetic images with realistic water wave surfaces. Simulations were effected on a shallow coastal region located in the East Coast of central Florida named Sebastian Inlet. This work was done in order to have a better understanding of what simulated reflectance can teach us. One should be able by changing bottom types, water quality and water depth to see difference in synthetic images as shown in the result section.

Realistic water Waves

Motion of fluids occurs in many forms. Surface water waves are easy to observe in imagery and their influence and impact on coastal, offshore structures, their implications on sediment transport, and coastal morphology as well as their momentum exchange between the atmosphere and the ocean makes them unique, complex and important to predict – perhaps from visible imagery. Over the years scientists and engineers have been trying to describe this phenomenon using mathematical equations based upon physical concepts and field data. Since Stokes and his contemporaries, a lot of theoretical work has been accomplished and understanding of water waves has advanced considerably. The models utilized can generate a discrete two-dimensional directional frequency spectrum of water waves. The generated 2D spectrum can then be used as input to generate realistic water wave surfaces. The spectral information of the power spectrum is used for the studies of ocean wave characteristics but also in order to design boats and to model waves for remote sensing applications. The statistical method of generating the spectrum is to represent the observed spectra by using two parameters, significant wave height and peak frequency. In general, sampled spectra show a large degree of variability, due in part to natural variations and resulting statistical fluctuations. Furthermore, the shape of wave spectra observed in water bodies varies considerably, even though the significant wave height and peak frequency are the same, depending on the duration and fetch of wind, stage of growth and decay of wind waves, and existence of swell. Therefore, sampled spectra and the representation of wave spectra by two parameters are insufficient to explain all characteristics of wave spectra in a specific area and periods. This makes a need for the parametric spectrums.

The parametric spectrum is expressed in terms of an analytical curve that preserves the feature of the observed spectra and includes a small number of physically meaningful parameters. Thus, because the parametric spectrum provides a continuous spectral information and more accurate representation of wave spectra, it is widely used to investigate the characteristics of spectra. Many parametric spectra of the form E(f), where E is the energy per unit bandwidth and f the frequency, have been proposed over the years ; among the best known are those of Pierson and Moskowitz (1964), Hasselmann et al. (1973), and Bouws et al. (1985). For fully developed wind waves in the open ocean, Pierson and Moskowitz (1964) proposed a form of the power spectrum (PM spectrum), which shows the fetch-independent form. Hasselmann et al. (1973) proposed the JONSWAP spectrum for the fetched-limited wind waves in the ocean. The additional factors in the JONSWAP spectrum allows for narrower, more peaked spectra which are typical forms of developing or "growing" seas in deep water. Bouws et al. (1985a) suggested a finite water depth spectral shape called the TMA spectrum to be applicable to wave conditions in shallow waters. The TMA spectral form has the additional parameter, water depth, "h" as well as the four JONSWAP parameters, the Phillips' constant, "a", the peak frequency, "f_m ", the peak enhancement factor, "r" and the spectral width factor, "sigma".

Frequency Spectrum

Pierson-Moskowitz spectrum

Pierson and Moskowitz (1964) assumed that if the wind blew steadily for a long time over a large area, the waves would come into equilibrium with the wind. This equilibrium state was named "fully developed sea". In order to generate a fully developed sea, a wind of 10m/s needs to blow with duration of 18 hours over about 320 km of ocean is needed. To obtain the spectrum of a fully developed sea, Pierson and Moskowitz used measurements of waves made by accelerometers on British weather ships in the North Atlantic. First, wave data were selected for times when the wind had blown steadily for long times over large areas of the North Atlantic, then wave spectra were calculated for various wind speeds. The Pierson-Moskowitz spectrum (valid for fully developed sea states) can be specified through the following parameters:

1- Wind speed 19.5 meters above the sea surface , $U_{19.5}$

2- Significant wave height, H_{m0}

3- Significant wave height, H_{m0}, and mean wave period H_{mean}

A Pierson-Moskowitz power spectrum is defined as:

$$S_{PM}(f) = A.f^5 \exp\left[-Bf^{-4}\right] \quad (3)$$

Where (when wind speed above the sea surface is known) $A = \frac{\alpha g^2}{(2\pi)^4}$, $B = 0.74\left(\frac{g}{2\pi U_{19.5}}\right)^4$, $\alpha = 0.0081$ is Phillips' constant (Komen et al. 1994), g = 9.81 gravitational acceleration.

Jonswap spectrum

The Jonswap spectrum is defined as:

$$S(f)_{Jonswap} = S_{PM}(f).\gamma^a \quad (4)$$

Where $S_{PM}(f)$ = Pierson-Moskowitz spectrum.
The shape parameters are defined as:

$$a = \exp\left[-\frac{1}{2}\frac{(f-f_p)}{\sigma f_p}\right]$$

$$\sigma = \begin{cases}\sigma_a \text{ for } f \le f_p \\ \sigma_b \text{ for } f > f_p\end{cases}$$

Where f_p denotes the peak frequency, γ = 3.3 (corresponding to standard Jonswap shape factor), $\sigma_a = 0.07$ (value corresponding to standard Jonswap spectrum), $\sigma_b = 0.09$ (value corresponding to standard Jonswap spectrum), where (when wind speed (10 meters above the sea surface)and effective fetch are known):

$$A = \frac{\alpha g^2}{(2\pi)^4}$$

where α is Phillips "constant" given by $\alpha = 0.0076\,\tilde{X}^{-0.22}$

The dimensionless fetch is defined by

$$\tilde{X} = \frac{gX}{u_{10}^2}$$

where X and u_{10} is the fetch and wind speed (10m above sea level)

$$B = \frac{5}{4}\frac{1}{T_p^4}$$

Where $f_p = 3.5\frac{g}{u_{10}}X^{-0.33}$, $f_p = \frac{1}{T_p}$

The TMA spectrum

The TMA spectrum is defined as:

$$S(f) = S(f)_{Jonswap} \cdot \phi(\omega_h) \quad (5)$$

Where $S(f)_{Jonswap}$ = Jonswap spectrum

$$\phi(\omega_h) \begin{cases} \frac{1}{2}\omega_h^2 & \text{for } \omega_h \le 1 \\ 1 - \frac{1}{2}(2-\omega_h) & \text{for } 1 < \omega_h \le 2 \\ 1 & \text{for } \omega_h > 2 \end{cases}$$

$$\omega_h = 2\pi f \sqrt{\frac{h}{g}}$$

h = water depth

Remote sensing is one of the many fields where the understanding of water waves is a key element affecting radiation transfer.. Remote sensing is defined as a technique of obtaining information about object through the analyses of data collected by specific instruments that are not in physical contact with the object studied. This science of "look but don't touch" has a wide application such as detection of hidden objects in ocean water as well as detection and analysis of imagery for water surface wave characterizations

3. SELECTED MODEL RESULTS

The side boundary of each pixel within the Monte Carlo model can play an important role in the final reflectance values obtained. Each pixel can be considered as a box (voxel) as shown in figure 1. The height is fixed with the water depth whereas the width of the box stays the same and is a personal choice.

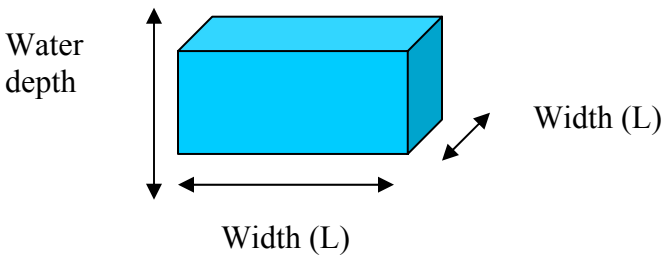

Figure 1. Representation of a pixel. The height represents the water depth and the voxel width (L) is fixed by the user.

By limiting the size of the width (L) we show the influence of L on reflectance due to tracking of photons out of and into the adjacent box. Changing "L" changes the final reflectance value observed as shown in figure 2 as expected. In order to quantitatively compare the reflectance values of the synthetic images, all the wave data points (pixels) in the red, blue and green channels or band were selected. Pixel by pixel and by wavelength or channel comparisons were made as shown in figure 3 and figure 4 for the HMCSIM. Figures 5 and 6 were used to compare the layered iterative model. Figure 3 and 4 are model results using the Phillips wave spectrum with a wind speed of 4 m/s and a wind direction of 90 degrees. The viewing angle is 90 degree and the solar angle is 90 degree to demonstrate an approach for pixel to pixel comparisons.

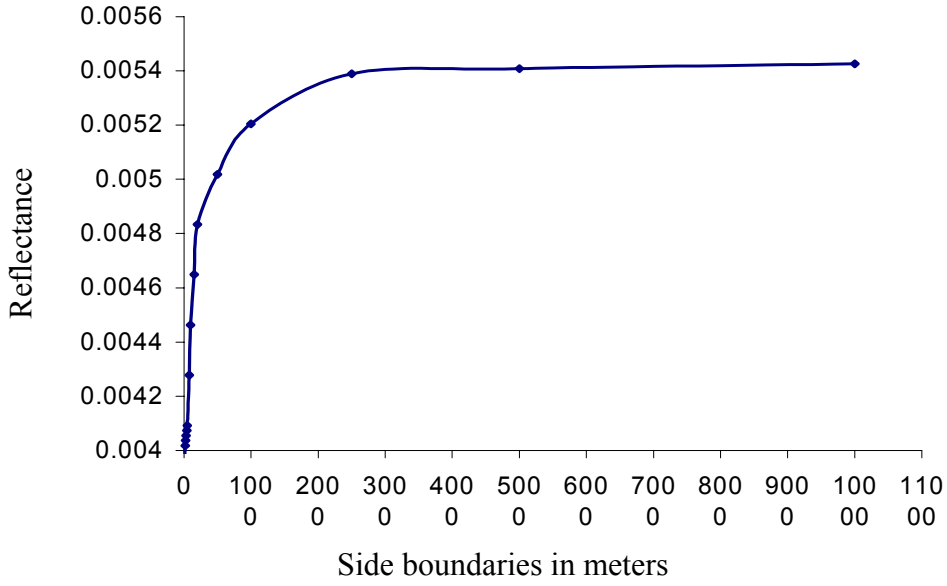

Figure 2. Change of reflectance (480 nm, 520 nm, 750 nm) values depending on the size of the voxel side boundaries (or width (L)) of the square pixels simulated in an image. This pixel was taken from a series of image and pixel values. The bottom type was sea grass. The chlorophyll a concentration is 1.0 mg/m^3 a dissolved organic concentration of 5.0 l/m^3 and a suspended sediments concentration of 0.05 g/m^3.

In order to quantitavely compare the reflectance values of the synthetic images, all the wave data points in the red, blue and green waveband were selected. The comparison was made by using figure 3 and figure 4 for the MCHSIM model. Figure 5 and 6 was used to compare the layered iterative model. Figure 3 and 4 are run using the Phillips wave spectrum with a wind speed of 4 m/s and a wind direction of 90 degree. The viewing angle is 90 degree and the solar angle is 90 degree as indicated above.

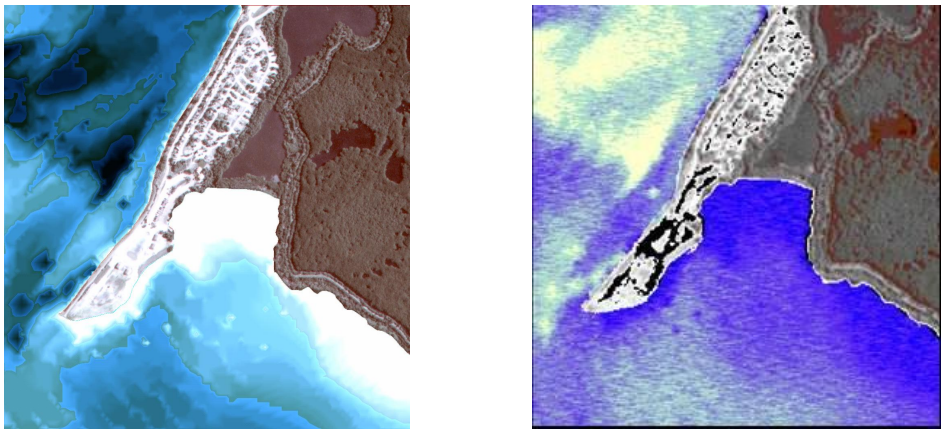

Figure 3 (left) Synthetic image (1000*1000) of Sebastian Inlet area generated using the layered iterative (LI) model. The bottom reflectance data is set at 0.1. Figure 4 (right) is a 1000*1000 synthetic image of Sebastian inlet area generated using the layered iterative model. Water waves using the Phillips spectrum are used. Wind speed is 4 m/s, wind direction 60 degree north, solar zenith angle is 90 degree and viewing zenith angle is 90 degree.

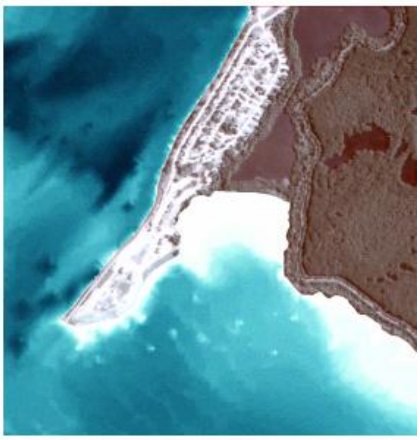

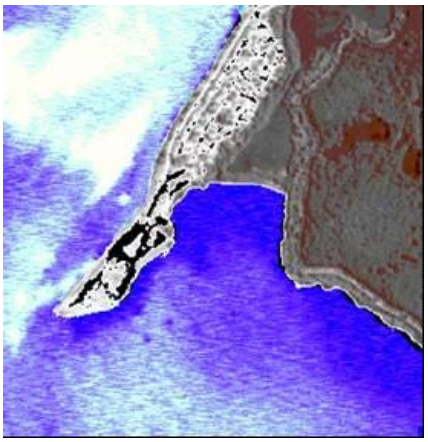

Figure 5 (left) Synthetic image (1000*1000) of Sebastian Inlet area generated using the Monte Carlo (MC) model. The bottom reflectance data is set at 0.1. Figure 6 (right) is a (1000*1000) synthetic image of Sebastian inlet area generated using the Monte Carlo model. Water waves using the Phillips spectrum are used. Wind speed is 4 m/s, wind direction 60 degree north, solar zenith angle is 90 degree and viewing zenith angle is 90 degree.

The following graphs (Figure 7 through 9) show a comparison of the iterative layered model (LI) versus the Monte Carlo model (MC). Future work and more calibration of the inputs of the models should reduce the current error of the three wavebands.

4. DISCUSSION & SUMMARY

The three statistical wave spectra used (Phillips 1958, Jonswap 1973 and Pierson-Moskowitz 1964) gave similar reflectance results. The comparisons of the models were tested using the simulated water wave images. The models were run with different wind speeds and wind directions as well as a change of the zenith solar and zenith viewing angle, and at different wavelengths. Simple animations were created and show that wind speed and direction is an important parameter for shallow water waves using the technique developed.

The results of the synthetic images can be considered realistic with the addition of different parameters such as water depth and bottom reflectance. It was observed that the following parameters need to be further considered in future model comparisons: the time of day the sensor passes over the study area, water quality concentrations, depth, solar and zenith angles, as well as atmospheric conditions. The generation of synthetic images requires a large amount of parallel computing time in the case of the Monte Carlo Model (Chang, 2002). By adding the realistic water surfaces to the existing two models a substantial improvement has been made in visual realism. The MC model requires a huge computation time even with the help of the FIT local Beowulf cluster with 48 processors in order to generate a hyperspectral cube. The analytical model however is fast and efficient. If for example, a hyperspectral synthetic image cube which has both high spectral and spatial resolution of 3 channels or bands needs to be generated, the 48 processor cluster takes several days of computation, whereas the analytical model takes only a few minutes to generate an image. Water depth, wind speed, wind direction and fetch are important parameters in order to create shallow water waves using a predefined wave spectrum. Parallel and related Grid computing will continue to be an

important tool to use with the MCHSIM model and will be necessary in our future applications of theses models to real life problems.

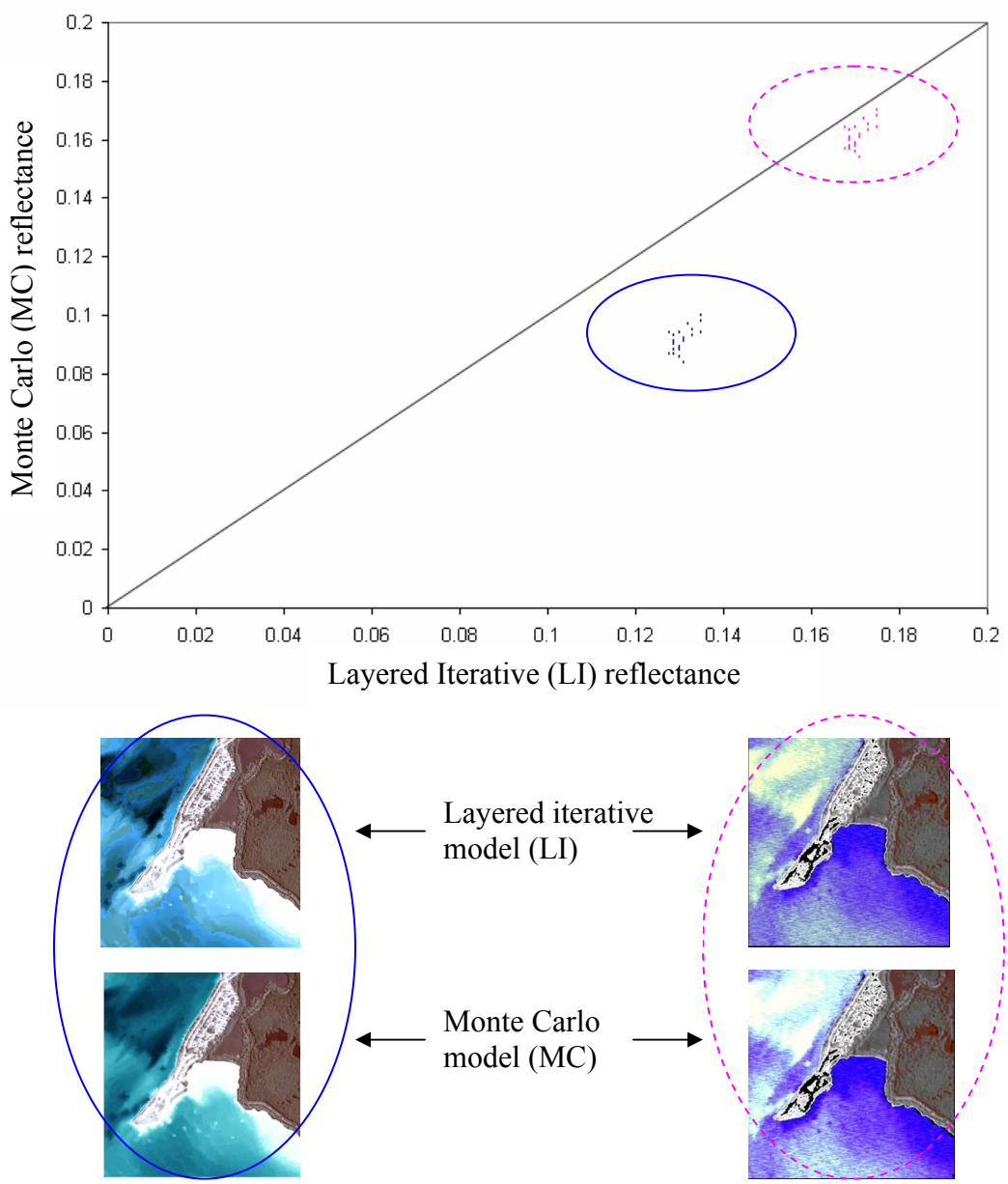

Figure 7 Comparison between the Monte Carlo (MC) model reflectance and the layered iterative (LI) model reflectance for the blue spectra (480 nm). The blue dot represent the original MC and LI model. The pink dots represent the MC model and the LI model with the new subroutine of water waves. The water is composed of SS= 0.05 g/m3, DOM= 5.0 g/m3. Chl-a= 1.0 g/m3.Wind speed 6 m/s, wind direction 90 degree, solar and zenith viewing angle are 90 degree. The Phillips wave spectrum is used.

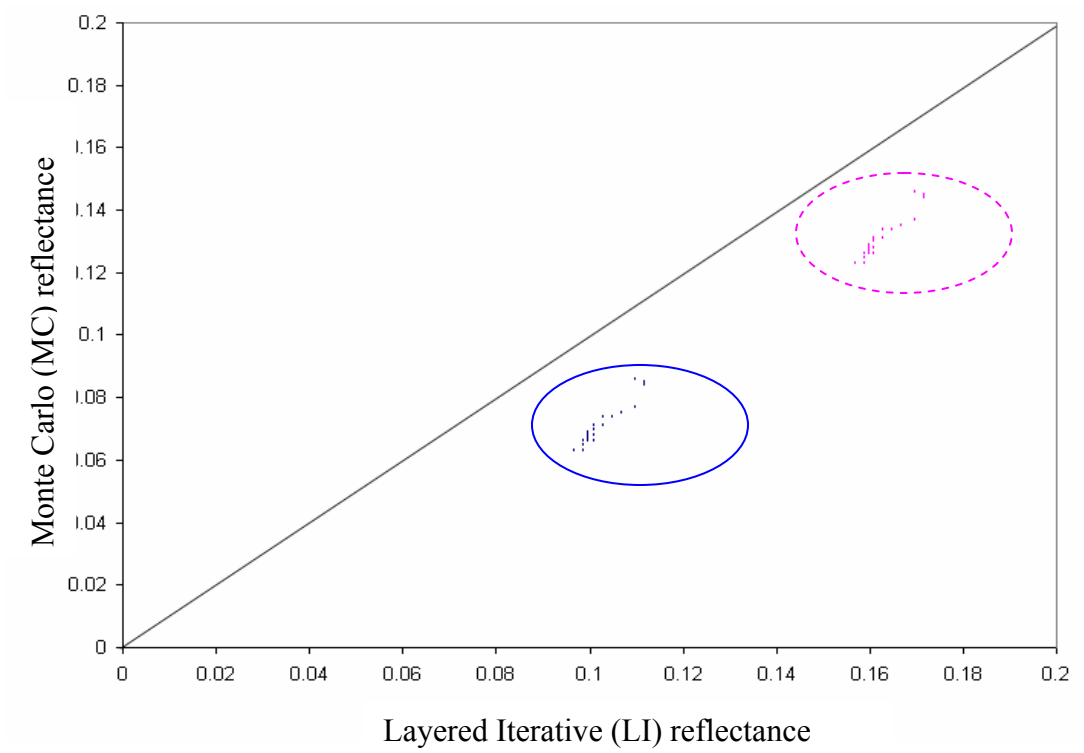

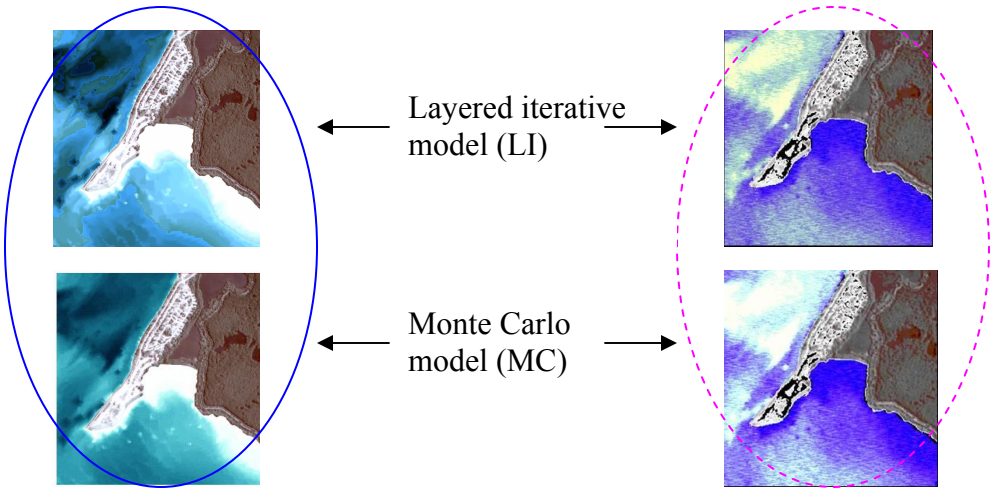

Figure 8 Comparison between the Monte Carlo (MC) model reflectance and the layered iterative (LI) model reflectance for the green spectra (520 nm). The blue dots represent the original MC and LI model. The pink dots represent the MC model and the LI model with the new subroutine of water waves. The water is composed of SS= 0.05 g/m3, DOM= 5.0 g/m3. Chl-a= 1.0 g/m3.Wind speed 6 m/s, wind direction 90 degree, solar and zenith viewing angle are 90 degree. The Phillips wave spectrum is used.

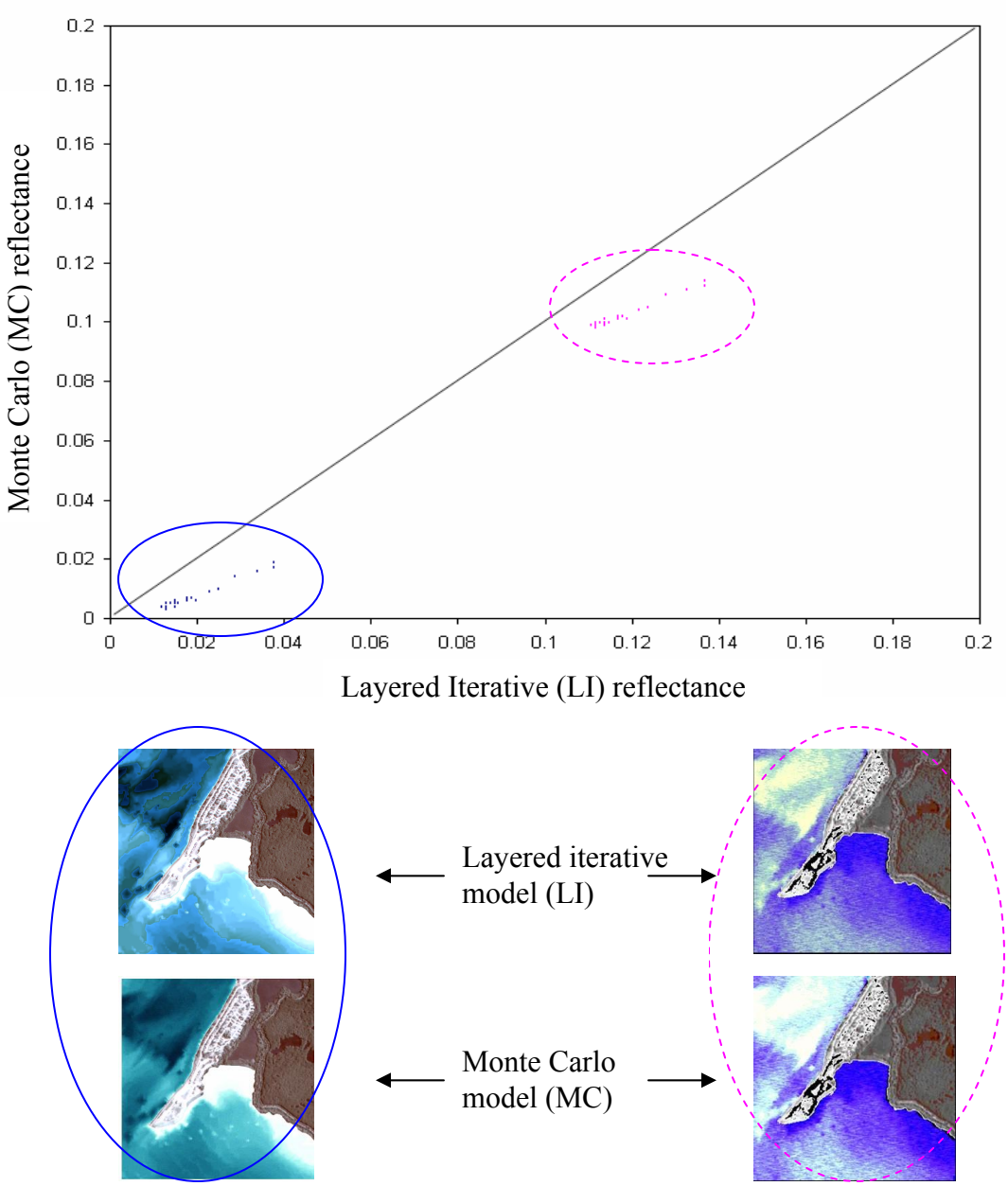

Figure 9 Comparison between the Monte Carlo (MC) model reflectance and the layered iterative (LI) model reflectance for the red spectra (650 nm). The blue dots represent the original MC and LI model. The pink dots represent the MC model and the LI model with the new subroutine of water waves. The water is composed of SS= 0.05 g/m3, DOM= 5.0 g/m3. Chl-a= 1.0 g/m3.Wind speed 6 m/s, wind direction 90 degree, solar and zenith viewing angle are 90 degree. The Phillips wave spectrum is used.

5. ACKNOWLEGEMENTS

The authors acknowledge the help of past students as well as support of NASA, NSF, US Dept. of Education, FIPSE, the State of Florida, St. Johns Water Management District, as well as the Link Foundation and Northrop Grumman Corporation for funding related to this project over the last several years to Florida Tech.

6. REERENCES

Preisendorfer, R., 1976, Hydrologic Optics, Honolulu, Hawaii; U. S. Department of Commerce, National Oceanic and Atmospheric Administration, Environmental Research Laboratories, Pacific Marine Environmental Laboratory.

Bostater, C., Chiang, G., Huddleston, L., Gimond, M., 2002, Synthetic Image Generation of shallow water using a parallelized Monte Carlo Hyperspectral Model or an Analytical Radiative Transfer Model. SPIE Vol. 4880, 16 pp.

Bostater, C., Ma, W., McNally, T., Gimond, M., Lamb, A., 1995, Application of an optical remote sensing model, In: Proceedings of the European Optical Society and SPIE – The International Society for Optical Engineering (EUROPTO), The European Symposium on Satellite Remote Sensing, Paris, France, Vol. 2586, 32-43 pp.

Tessendorf, J., Simulating Ocean Water, SIGGRAPH 2001 Course notes, http://home1.gte.net/tssndrf/index.html, 19 pp.

Bostater, C., and Huddleston, L., 2000, Layered analytical radiative transfer model for simulating water color of coastal waters and algorithm development, In: Proceedings of the European Optical Society and SPIE – The International Society for Optical Engineering (EUROPTO), Remote Sensing of the Ocean and Sea Ice 2000, Barcelona, Spain, Vol. 4172, 153-161 pp.

Bostater, C., Huddleston, L., and Tepel, M., 2001, Improvements to a layered analytical irradiance model for application to coastal waters with depth dependent water constituents, various bottom types, and variable water depths, In: Proceedings of the European Optical Society and SPIE – The International Society for Optical Engineering (EUROPTO), Remote Sensing of the Ocean and Sea Ice 2001, Toulouse, France, Vol. 4544, 236-245 pp.

Bostater, C., Huddleston, L., Semmler, C., and Mieles, J., 2002, "An iterative algorithm for layered optical remote sensing reflectance modeling of natural waters with depth dependent aquatic constituent concentrations," In: Proceedings of the European Optical Society and SPIE – The International Society for Optical Engineering (EUROPTO), Remote Sensing of the Ocean and Sea Ice 2002, Agia Pelagia, Crete, Greece, Vol. 4880, 88-101 pp.

Bostater, C., Huddleston, L., Bassetti , L., 2003, Hyperspectral synthetic image generation of shallow water using an analytical layered radiative transfer model with realistic water surface waves" Proceedings of the European Optical Society and SPIE – The International Society for Optical Engineering (EUROPTO), Remote Sensing of the Ocean and Sea Ice 2003, Barcelona, Spain, Vol. 5233, 253-268 pp .

Phillips, O., 1958, The equilibrium range in the spectrum of wind-generated waves. Journal of Fluid Mechanic., Vol. 4, 426-434 pp.

Pierson, W., and Moskowitz, L., 1964, A proposed spectral form for fully developed wind seas based on the similarity theory of S.A. Kitaigorodskii. Journal of Geophysical Research, Vol. 69**,** 5181-5190 pp .

Pierson, W., and Marks W., 1952, The power spectrum analysis of ocean-wave records. Trans. Amer. Geophys. Union., Vol. 33, 6, 834-844.

JONSWAP Group, 1973, Measurements of wind-wave growth and swell decay during the Joint North Sea Wave Project (JONSWAP). Deut. Hydrogr. Z. A12.

Phillips, O., 1958, The equilibrium range in the spectrum of wind-generated waves. Journal of Fluid Mechanic., Vol. 4, 426-434 pp.

Hasselmann, K., Barnett, T., Bouws, E., Carlson, H., Cartwright, K., Enke, J., Ewing, H., Gienapp, D., Hasselmann, P., Kruseman, A.,Meerburg, P., Müller, D., Olbers, K., Richter, W., Walden, H., 1973, Measurements of wind-wave growth and swell decay during the Joint North Sea Wave Project (JONSWAP), Dtsch. Hydrogr. Z., 8 (suppl. A). 19 pp.